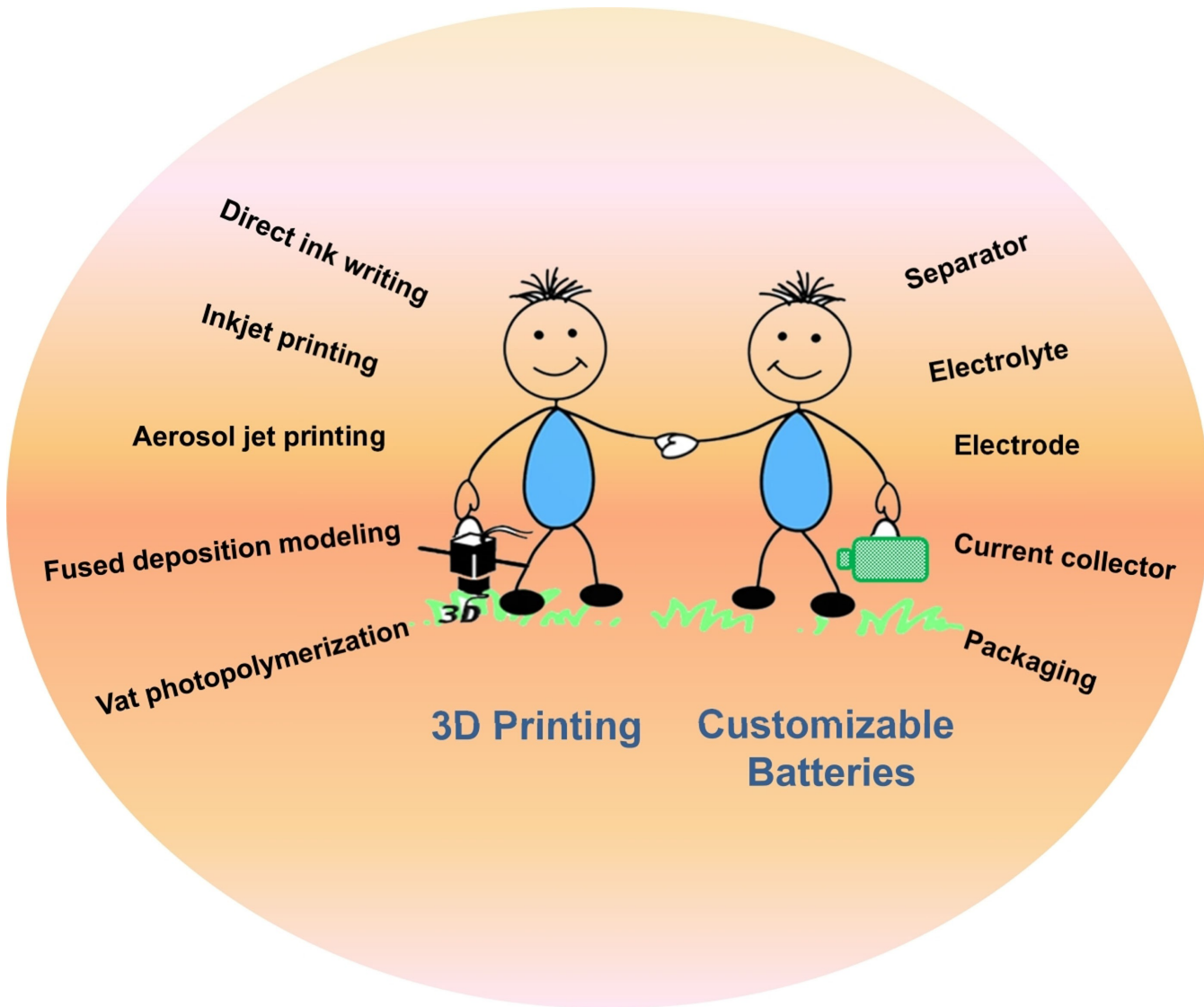


3D Printing Enables Customizable Batteries

Huifa Shi,^[a, c] Jiakai Cao,^[a, c] Zhenhua Sun,*^[b] Zahid Ali Ghazi,^[d] Xiaoyang Zhu,^[a] Sa Han,^[a, c] Danyang Ren,^[e] Guixia Lu,^[f] Hongbo Lan,*^[a] and Feng Li*^[b]



3D printing, as a new technology, brings great freedom in the design and manufacturing of batteries. It offers unique advantages by the production of more advanced batteries with specific properties, such as good internal structural controllability, high shape conformability, and enhanced power capability and energy density. In this review, we provide an overview of 3D printing technologies in the field of customizable batteries. First, we introduce fundamental concepts of customizable batteries and the distinct advantages of 3D printing. Then, five representative 3D printing techniques are discussed

along with their operating mechanisms, requirements for printing materials, manufacturing accuracy, and technical features. In addition, from the perspective of the three basic levels (pore structure, component architecture and interface, as well as battery appearance and mechanical deformability) of customizable batteries, a detailed overview is provided to gain an in-depth understanding. The state-of-the-art developments and current major challenges are summarized and discussed. Finally, potential research area is proposed to utilize 3D printed customizable batteries for practical applications.

1. Introduction

With the popularization of portable electronics and electric vehicles, rechargeable batteries have emerged as candidates for next-generation energy storage systems. In the future, their application will be extended to other devices, such as the Internet of Things,^[1] wearable electronics^[2] and electronic skin.^[3] Consequently, next-generation batteries not only require high energy density, long lifetime and high safety, but also emphasize customization and miniaturization. To date, intensive research efforts have focused on the discovery and regulation of electrode/electrolyte materials, and significant progress has been made in basic theory and electrochemical performance improvement.^[4,5] However, the manufacturing technology of batteries is much less diversified, and new technologies and processes is insufficient. Commercial lithium-ion batteries and potential post-lithium-ion batteries are still manufactured by slurry-coating process, which includes slurry preparation, tape casting, component winding or stacking and packaging.^[6] This manufacturing process is standardized and

well modularized, making it suitable for low-cost, high-volume production. However, its design freedom is very limited, making it difficult to customize the component architecture, configuration, and battery appearance as required. Therefore, there is an urgent need to develop more advanced manufacturing technology to meet these requirements.

Three-dimensional (3D) printing, an emerging specialty technology in additive manufacturing, is a rapidly emerging and innovative field of research. With the help of the computer-aided design, it is possible to fabricate the desired 3D objects with any geometry (e.g., porosity, dimension, and morphology).^[7] As shown in Figure 1(a), a typical 3D printing process is as follows. First, the software is used to create a virtual 3D model of the target object. Then, the 3D object is sliced into many two-dimensional horizontal cross-sections. The third step is to realize successively layer-by-layer material printing with a 3D printer. Finally, after post-processing, the target object is obtained. In terms of its technical characteristics and manufacturing process, 3D printing is competitive in terms of production efficiency, process automation, precision control, cost, etc.^[8] Therefore, it has been widely explored in the fields of transportation,^[9] aerospace,^[10] industrial equipment,^[11] consumer electronics^[2] and healthcare.^[12] More importantly, compared with conventional technologies, 3D printing has inherent advantage of customizable and controllable structural prototyping, enabling versatile and demand-oriented architecture designs.

Over the past decade, 3D printing technology has found applications in a wide range of energy storage devices, particularly rechargeable secondary batteries. In the battery manufacturing process, eight metrics need to be focused on, including energy density, power density, large-scale manufacturing capability, design freedom, process complexity, device miniaturization, technical accuracy, and manufacturing cost (Figure 1b). Although 3D printing cannot compete with the blade-coating method in terms of production efficiency and cost at this stage, it still exhibits outstanding advantages in the design freedom, low process complexity, device miniaturization and high technical accuracy. Diverse and efficient electrode/electrolyte architectures fabricated using 3D printing technology improve the surface-to-volume ratios and shorten the electron and ion transport distance, resulting in improved energy/power density of the devices. Therefore, 3D printing is a

- [a] Prof. H. Shi, J. Cao, Prof. X. Zhu, S. Han, Prof. H. Lan
Shandong Engineering Research Center for Additive Manufacturing
Qingdao University of Technology
Qingdao 266520 (China)
E-mail: hblan99@126.com
- [b] Prof. Z. Sun, Prof. F. Li
Shenyang National Laboratory for Materials Science
Institute of Metal Research
Chinese Academy of Sciences
Shenyang 110016 (China)
E-mail: zhsun@imr.ac.cn
fli@imr.ac.cn
- [c] Prof. H. Shi, J. Cao, S. Han
Key Lab of Industrial Fluid Energy Conservation and Pollution Control
(Qingdao University of Technology)
Ministry of Education
Qingdao 266520 (China)
- [d] Dr. Z. A. Ghazi
National Centre of Excellence in Physical Chemistry
University of Peshawar
Peshawar, 25120, Khyber Pakhtunkhwa (Pakistan)
- [e] D. Ren
Research Center for Hybrid Sensing
Zhejiang Laboratory
Hangzhou 311100 (China)
- [f] Dr. G. Lu
School of Civil Engineering
Qingdao University of Technology
Qingdao, 266033 (China)



Huifa Shi received her PhD in materials science and engineering from Tsinghua University in 2010. Now, he is an associate professor at Qingdao University of Technology. His research interests include micro/nano-scale 3D printing and its applications in energy storage batteries.



Jiakai Cao obtained his bachelor's degree in 2021 from West Anhui University, and is a Master's degree candidate of Qingdao University of Technology. His research interests focus on the 3D printing and its application in the aqueous zinc-ion batteries.



Zhenhua Sun received his B.S. and Ph.D. degrees in inorganic chemistry from Jilin University in 2001 and 2006, respectively. He was then a Postdoctoral Research Fellow at the Chinese University of Hong Kong from 2007 to 2009. He is currently a Professor at the Institute of Metal Research, Chinese Academy of Sciences. His current research interests mainly focus on the carbon-based composite materials for electrochemical energy storage. He has published more than 110 papers in peer-reviewed journals including Chemical Society Reviews, Nature Communications, and Advanced Materials with more than 10000 citations (H-index 50).



Zahid Ali Ghazi received his Ph.D. degree from National Center for Nanoscience and Technology, Beijing-University of Chinese Academy of Sciences (NCNST-UCAS) in 2017 followed a postdoc with Professor Feng Li at the Institute of Metal Research, Chinese Academy of Sciences (IMR, CAS). Currently, he is working as an Assistant Professor at National Centre of Excellence in Physical Chemistry, University of Peshawar, Pakistan. His research interests focus on functional nanomaterials for electrochemical energy storage systems, such as lithium metal batteries, lithium sulfur batteries, and supercapacitors.



Xiaoyang Zhu is an associate professor of Shandong Engineering Research Center for Additive Manufacturing at Qingdao University of Technology. He received his Ph.D. degree in Mechanical Engineering from Nanjing University of Science and Technology in 2016. His research interests are micro-scale 3D printing, multi-scale and multi-material 3D printing, transparent electronics, flexible electronics, conformal electronics, and multilayer electronics. He holds 20 patents and published 50 papers.



Sa Han obtained his bachelor's degree in 2021 from Lanzhou University of Technology. Now, she is a Master's degree candidate of Qingdao University of Technology. Her research interests focus on the development of advanced materials and electrodes for lithium sulfur batteries.



Danyang Ren received her Master's degree in State Key Laboratory of New Ceramics and Fine Processing, Tsinghua University in 2019. She received her bachelor's degree in materials science and engineering in 2016. After graduating in 2019, she went to Shenzhen BYD Lithium Battery Co., Ltd. as a senior development engineer, engaged in the research of active material materials and polymer separator materials for lithium batteries. From May 2020, she worked as an engineer in Zhejiang Lab, Hangzhou, China. And she mainly engaged in the research of composite piezoelectric materials and the manufacture of ultrasonic transducers.



Guixia Lu received her Ph.D. degree from Shandong University in 2015 and now works in Qingdao University of Technology. In 2019, she went to the University of New South Wales in Australia as a CSC sponsored visiting scholar. Her main research interests are the synthesis and application of composite materials for electrochemical energy storage.



Hongbo Lan is a professor and a director in Shandong Engineering Research Center for Additive Manufacturing, Qindao Engineering Research Center for 3D Printing, Qingdao University of Technology. His research interests include micro/nano-scale 3D printing, additive manufacturing advanced circuits and electronics, large-area nanoimprint lithography, additive manufacturing. He is the author and co-author of 1 book, 6 book chapters, over 150 scientific papers in journals and conferences. He held 52 China granted patents, 3 U.S. granted patents and 1 German granted patent. He was elected as national outstanding middle-aged and young expert, has received special government allowances of the State Council.



Feng Li is Professor of both the Advanced Carbon Research Division of Shenyang National Laboratory for Materials Science, Institute of Metal Research, Chinese Academy of Sciences (IMR, CAS), and University of Science and Technology of China. He received his PhD degree in materials science at IMR, CAS. His main research interests focus on the nanomaterials for electrochemical energy storage and conversion, including lithium-based batteries and electrochemical capacitors. He currently has published more than 300 peer-reviewed papers with more than 45000 citations. He is recognized as a highly cited researcher by Clarivate Analytics.

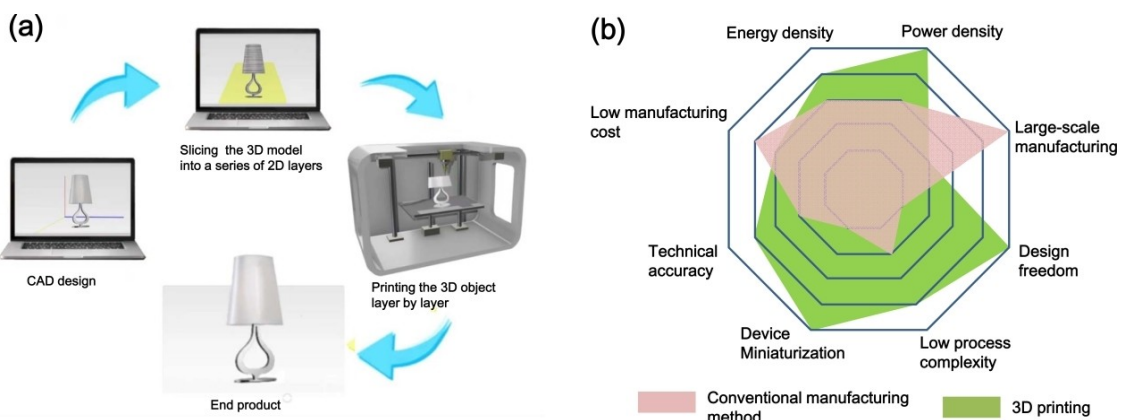


Figure 1. a) Illustration of the 3D printing process. b) Conventional battery manufacturing method versus 3D printing method.

better option for creating customizable batteries for future wearable devices.

In recent years, the production of customizable batteries through 3D printing has gained increasing attention. To provide an overview of the evolving state of the field, this review first analyzes the fundamental concepts of customizable batteries and the unique advantages of 3D printing. Then, five commonly used 3D printing techniques for the fabrication of customizable batteries are introduced. Next, the latest advances of 3D printing in customizable batteries are discussed in detail, including interior pore structures, component architecture and interfaces, as well as device appearance and mechanical properties. Finally, the status and future challenges in the development of customizable batteries through 3D printing will be discussed.

2. Fundamental Concepts and Unique Advantages of 3D Printing

Normal battery manufacturing processes can only produce rigid laminated structures, which are also easily damaged by various deformation processes, such as cracking, relaxation,

and distortion. When the electrode thickness increases, ions/electrons need to move long distances in the vertical direction of the electrode, which seriously affects their high power performance. In addition, the geometry of cells is limited to several common shapes, such as cylinders, coins, and pouches. In modern electronic products, the battery must not only serve as a power source, but also be customizable according to product requirements and application scenarios. As for the customizable batteries by 3D printing, there are three levels of elements (Figure 2). First, at the pore structure level within the electrode, the pores of the active material/electrode should be purposefully designed and created, including pore sizes, pore types, pore shapes, pore distribution, pore volume, etc., to ensure the rapid infiltration of the electrolyte and the unimpeded ion/electron transport. It should be recognized that pore structure also has a direct impact on the volumetric energy density of the cell. Second, at the functional component level, the component architectures (electrodes, electrolytes, separators, etc.) are no longer confined to the 2D plane, but to the 3D structure, and the contact interface between components is supposed to be purposefully optimized. The result is an increase in the surface-to-volume ratios and a shortening of the transport distance of electrons/ions, for example, through an interdigitated structure. Batteries made in this way usually

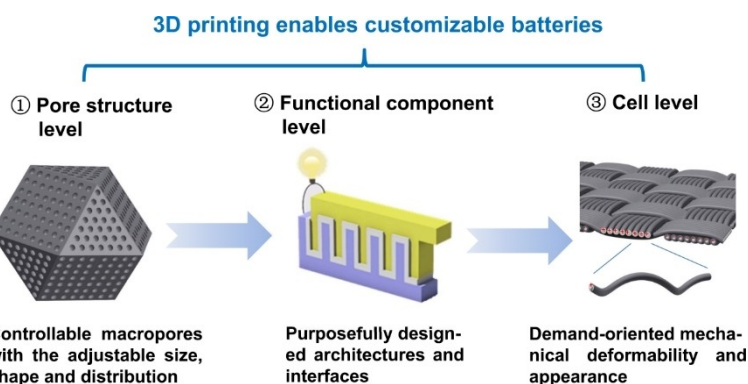


Figure 2. Three levels of key elements regarding customizable batteries by 3D printing: pore structure level, functional component level and cell level.

feature high power density and high mass loading of active materials. Third, at the cell level, the mechanical deformability and appearance must be customizable according to the application scenario. For example, batteries used in an electronic fabric must have a fibrous shape and can be woven. When used in smart glasses and electronic skin, the batteries should be able to adaptably cover the surface of the target objects.

3D printing is an effective technology to produce customizable batteries. In particular, the development of the Internet of Things has continued to drive development in this field. Several notable advantages of 3D printing include the following: (1) Based on designed printing paths, 3D printing allows precise control of the size, shape and distribution of macropores on the micrometer scale. In the electrode, these large pores effectively accommodate the electrolyte and provide fast electron transport paths. (2) 3D printing can be used to fabricate a wide range of complex and targeted architectures, such as interdigitation, 3D scaffold fiber and concentric micro-pillar array. These innovative architectures have a large electrode-electrolyte interface and shorter ion diffusion length. As a result, the printed batteries can achieve maximized energy/power densities.^[13] Moreover, with the planar interdigitated structure, it is easy to integrate numerous cells by 3D printing. (3) Depending on the specific application scenarios and the requirements of target customers, the appearance of batteries can be customized by 3D printing. Furthermore, 3D printing is capable of conformally manufacturing and packaging batteries on non-planar substrates with complex surface topologies, such as spherical surfaces and curved structures. (4) The individual components (electrode, electrolyte, current collector, separator, and packaging) could be printed sequentially and integrated directly into an entire battery, bringing the

benefits of simplified processing and energy savings. Moreover, the minimal material wastage helps to reduce production costs.^[13,14]

3. Printing Technologies and Material Selection

Depending on the principle of operation, 3D printing technologies are classified into seven categories by the American Society for Testing and Materials, including (1) material extrusion, such as direct ink writing (DIW) and fused deposition modeling (FDM), (2) vat photopolymerization (VPP), such as stereolithography, digital light processing (DLP), and two-photon lithography (TPL), (3) material jetting, such as inkjet printing (IJP) and aerosol jet printing (AJP), (4) powder bed fusion, (5) sheet lamination, (6) binder jetting and (7) directed energy deposition.^[13] However, not all 3D printing technologies are compatible with the manufacturing of customizable battery. In this section, the five most used techniques (Figure 3) are presented and compared. All five printing techniques offer high design flexibility and enable the fabrication of complex objects. However, these printing techniques have different working principles, resulting in differences in printable materials, ink requirements, printing accuracy and so on.

3.1. Direct ink writing

DIW is a typical extrusion deposition process (Figure 3a), which is broadly divided into three main steps, including ink preparation, execution, and solvent removal.^[15] First, the printable material and the solvent are mixed to obtain an ink with appropriately high viscosity and elastic behavior. Second,

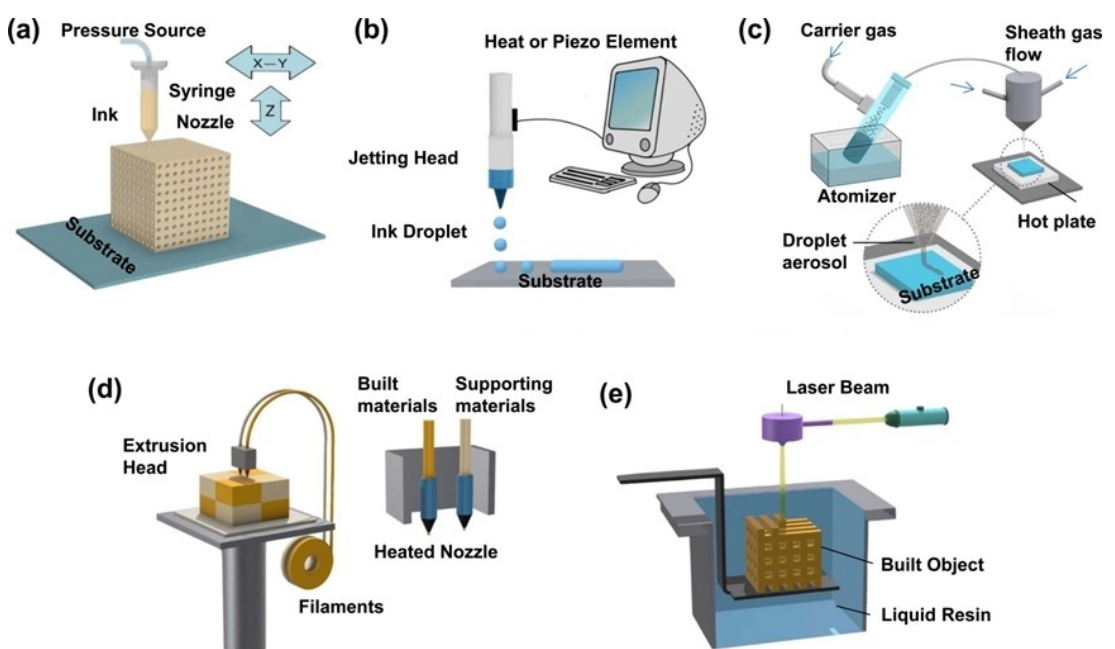


Figure 3. Schematic illustration of five representative 3D printing techniques: a) DIW, b) IJP, c) AJP, d) FDM and e) stereolithography.

the prepared ink with good printability is loaded into a syringe and extruded through a nozzle with the help of suitable pressure. The resulting continuous filaments are solidified on the moving platform. Finally, the solvents are removed from the printed architectures. To ensure a stable squeezing process and high printing accuracy, special attention should be paid to optimizing the rheological properties of the ink, such as viscoelastic properties (i.e., loss and elastic moduli), apparent viscosity, and yield stress under shear and compression. The proper rheological behavior ensures smooth extrusion of inks from tiny printing nozzles with characteristic size ranging from microns to millimeters.^[16] At a low applied pressure, an ideal ink should resemble a solid with a non-flowing form. Once a proper stress is applied, the ink can fluently flow as a viscous liquid.^[17] Usually, thickening agents such as graphene oxide^[18] and celluloses^[19] are added to inks to regulate the rheology of the ink.

Unlike other 3D printing technologies, DIW is a relatively simple process and is not limited by material categories. Therefore, almost all functional active materials can be made into printable inks.^[17] Moreover, the printable ink only needs a small amount of thickener, which will not affect the electrochemical activity of the functional components. In addition, by extruding different ink materials simultaneously, DIW enables one-step printing of multi-material structures. For these reasons, DIW is the most popular technique for the electrode, electrolyte, current collector and separator manufacturing. By external stimulants (electromagnetic waves, acoustic waves, magnetic fields and heat sources, etc.), the printing conditions/setup can be easily changed, which facilitates the fabrication of 3D structures with high precision and aspect ratio.^[20]

3.2. Inkjet printing

IJP is a droplet ejection-based technique widely used in daily document printings (Figure 3b). In this technique, the prepared ink is stored in a syringe. A heat or piezo element is connected to the nozzle, which creates a pressure that forces the ink to quickly flow out of the nozzle and deposit on the substrate.^[21] The motion trajectory of the nozzle is controlled to obtain a pre-designed pattern. In terms of working principles, IJP is divided into continuous mode and drop-on-demand mode. In the continuous mode, the ink droplet is electrostatically charged and continuously ejected. Depending on the established printing path, the ink droplets are deposited onto the substrate or a recycling box under the influence of an electric field. However, for a drop-on-demand mode, the ink droplets are ejected onto a substrate as needed, which is controlled by software.^[22] To achieve a high-quality printing, the prepared inks must meet several specific requirements, such as low viscosity, low surface tension, free-agglomeration, and good flowability.^[23]

Usually, the nozzle used for IJP has a small diameter (< 5 µm) ensuring high resolution, which is well suited to printed electronics. Like DIW, the printable ink for IJP is compatible with a variety of battery materials. However, the thickness

printed by IJP is largely limited, indicating that the available patterns are confined to the 2D L surface. Therefore, IJP is more suitable for the fabrication of planar and ultra-thin electrode, electrolyte separator and current collector.

3.3. Aerosol jet printing

Aerosol printing is also a subclass of material jetting. As shown in Figure 3(c), the functional ink is aerosolized by two optional methods: pneumatic atomization and ultrasonic atomization. Small droplets with the diameters of 1–5 µm are entrained in the carrier gas while larger droplets (>5 µm) are deposited back into the ink reservoir under the action of gravity. The droplet aerosol is transported to the deposition nozzle. Inside the deposition nozzle, the aerosol encounters another annular sheath gas flow. When the sheath gas and the aerosol pass through the deposition nozzle at the same time, the mixture is compressed and ejected. The resulting high velocity converging particle stream is deposited in well-defined locations. The main factors affecting printing resolution include needle diameter, sheath gas flow rate, carrier gas flow rate and ink quality (surface tension, solids loading and viscosity).^[24]

AJP is capable of printing a variety of materials, including metals, polymers, ceramics, et al. More importantly, AJP has a flexible working distance of 1–5 mm between the deposition nozzle and the substrate, making it applicable for the material deposition on non-planar substrates with multiscale surface topologies.^[25,26] Therefore, AJP is ideal for conformal printing of the current collectors, electrodes, and electrolytes on any object surface.

3.4. Fused deposition modeling

FDM, also known as fused filament fabrication (Figure 3d), was first introduced and commercialized by Stratasys in the 1990s.^[27] By depositing materials in a layer-by-layer way, FDM is able to produce complex prototypes. Before printing, thermoplastic filaments are prefabricated by a polymer extruder. The obtained filaments are transported into a liquefied head and converted into a semi-molten state by the controlled temperature (150–300 °C).^[28] The materials are then extruded through a nozzle and deposited on a building platform. The semi-molten material is then cooled and solidified. Tracing the cross-sectional shape of the prototypes with computer-aided design data, the extrusion nozzle moves levelly through the established trajectories to make a uniform layer. The platform moves down by one unit distance, and another layer is produced by repeating the above-mentioned process.^[27] Two types of thermoplastic materials are required for FDM to produce 3D prototypes with cavity and cantilever structures, including built materials and supporting materials. The built materials (butadiene, styrene, polyethylene, polypropylene and wax, poly(lactic acid), etc.) are used to build the prototype body, while the supporting materials (water-soluble materials and

peelable materials) are peeled off and removed after modeling.^[29]

Because of the unique technology principle of FDM, active materials of the electrode/electrolyte are required to be mixed with thermoplastic materials in advance. The mass fraction of thermoplastic materials is often larger than 50 wt.%,^[30,31] which inevitably blocks the electron/ion pathways and reduces the mass energy density of the battery. In general, FDM is more suitable for printing chemically inert and lightweight packaging and separator.^[32]

3.5. Vat photopolymerization

In VPP, photosensitive resin is selectively irradiated with ultraviolet light and cured, and a complete device is fabricated by stacking multiple layers (Figure 3e). Depending on the irradiation method, VPP is generally divided into stereolithography, digital light processing (DLP) and two-photon lithography (TPL).^[33] In stereolithography, the built platform is covered with a layer of photosensitive resin. Photopolymerization is initiated by irradiating the cross-section of the target with ultraviolet light, which is controlled by software. In this way, the liquid monomers solidify spontaneously. The built platform is moved down one layer, and a new layer of liquid monomers is blade-coated on the top surface. Elaborated objects can be carried out by repeating the above light-curing steps. Finally, the wet uncured resin is cleaned with ethanol. The DLP process is similar to stereolithography, but allows light to be projected onto the surface with a specific contour. The corresponding resin areas are all cured at once. Therefore, it has a higher formation efficiency. In TPL, the resin is cured occurs by the intersection of two-photons, which allows greater printing accuracy and higher production rates.^[34]

Like FDM, the printable materials in VPP need a lot of photosensitive resin. Usually, the resulting polymer scaffold cannot be used directly as an electrode/electrolyte, but is often used as a precursor for electrode/electrolyte preparation or as a supporting skeleton to carry the active materials.^[35,36] In addition, VPP is also used for the manufacture of battery packaging.^[37]

3.6. Technique comparison and their applicability in customizable batteries

A customizable battery mainly consists of cathode/anode, current collector, separator, electrolyte, and packaging, each of which is made of a completely different class of material. Besides, each component has different technological requirements. For example, electrodes and separators usually require a certain porosity to allow for smooth ion transport. The outer packaging layer is used to isolate air and water, so it needs to be particularly dense. In general, three key points need to be considered when the printing technique is chosen. First, prior to printing process, it is essential to ensure that the materials required for the component can be converted into compatible

inks or materials with the chosen technique. Moreover, the inactive component in the inks cannot be excessive. Second, the process should not destroy the functional properties of the materials, especially the electrochemical activity of the electrode materials. Third, the chosen technique must meet the technical requirements for printing the component, including resolution, structural diversity, multi-material capability, etc. Therefore, to achieve high quality battery and its component printing, the key performance metrics of the various techniques should be fully considered.

DIW has excellent multi-material manufacturing capabilities, and moderate printing resolution of 1–250 µm. In addition, it can realize the rapid printing of diverse structures, so it is the most widely used in the printing of battery components. However, DIW has high requirements on viscoelasticity of used inks, and low-viscosity inks are usually nonprintable. After printing, post-processing is often required to remove the solvent and solidify the structure. The used ink in IJP is similar to that in DIW, but has a lower viscosity (40–100 cp). It is also suitable for multi-material printing, and the printing cost is lower. But printing structures are often limited to 2D planes with a resolution of 5–200 µm. Compared to IJP, AJP has much higher printing resolution (~10 µm) and alignment precision (< 2 µm). The required inks have a wide viscosity requirement of 1–1000 cP. In addition, it has a significantly improved resilience to clogging.^[38] FDM is a perfect tool to realize desired electrodes or electrolytes directly, and the complex and difficult ink preparation process can be avoided.^[39] However, FDM requires the addition of a large quantities of thermoplastic materials in the manufacturing process, which will reduce the energy density of the battery. In addition, FDM operating conditions require high temperature, which may destroy the active component of the electrodes/electrolytes. The precision of FDM printing needs to be further improved,^[8] especially along the Z-axis with a resolution of 200 µm for the first layer and 50 µm for the sequential layers.^[39] VPP technology can produce complex electrode/electrolyte architecture with high precision (0.2–10 µm), and high efficiency. Meanwhile, the resulting pore structure can be continuously and precisely regulated. In addition, since the monomer is already in a liquid state, heating of the polymer feed and nozzle is avoided. However, VPP involves high equipment maintenance and operation costs, which limits its commercialization. There are only a limited number of compatible photopolymers, and the photosensitive resin is brittle after curing and can easily break during processing. As described above, the different printing techniques have its characteristics in terms of raw materials, ink preparation, printing resolution, etc. The relevant comparisons in terms of the key performance indicators are summarized in Figure 4.

4. Customizable Interior Pore Structures

The pore structure in a battery, especially the electrode component, is a key parameter, greatly affecting the active area of the reaction, electrolyte infiltration, mass transport rate and

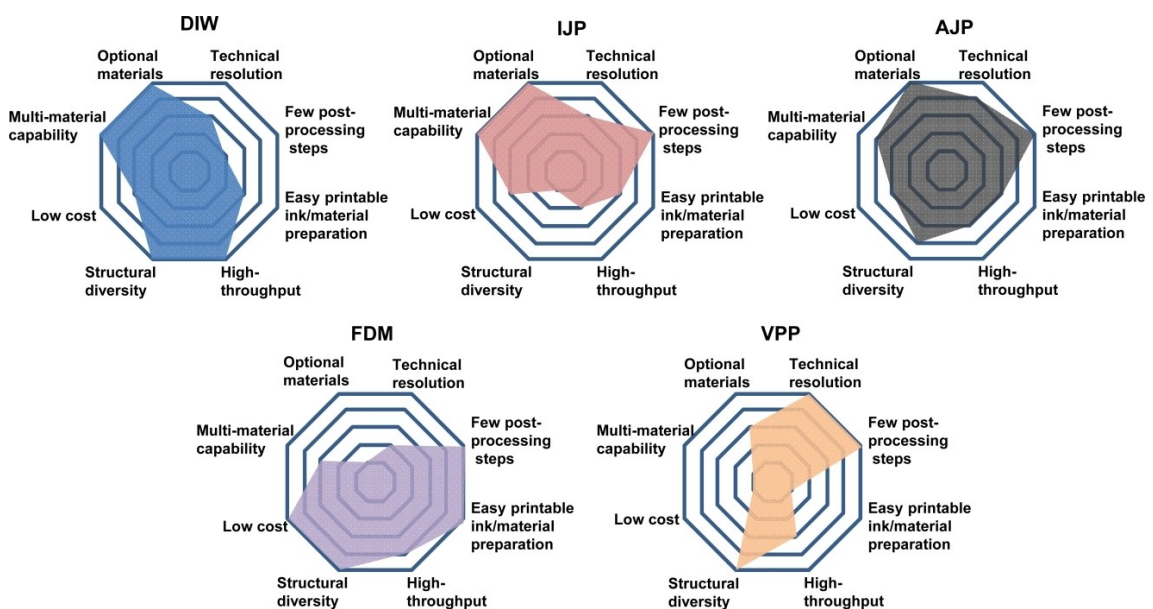


Figure 4. Radar plots comparing key performance metrics for the different 3D printing techniques in customizable battery manufacturing.

accommodation of the active materials. Customization of pore structures refers to creating pores with specific size and shape according to the reaction requirements, and further regulating the proportion and distribution of different types of pores. In 3D printing, customizing pore structures covers two aspects: periodic open macropores by printing and hierarchical pores by pre-/post-processing.

As mentioned above, 3D printing can realize the accurate manufacturing of arbitrary structures over the micro-meter scale. A typical example is the periodic open macropores or holes in a 3D skeleton. In the vertical and planar directions of electrodes, the naturally interconnected pores between adjacent filaments are formed. Compared with the conventional electrodes having inhomogeneity and tortuous pores.^[40] These open macropores specially created by 3D printing significantly reduce the pore tortuosity in the electrode, facilitating the electrolyte smooth infiltration and the unhindered ion transport. Moreover, ionic transport paths are shortened. As a result, the obtained batteries in the literature usually emphasize the superiority of high loading and excellent power output.^[41–43] For example, Kaner et al.^[44] fabricated carbon frameworks by stereolithography that were used as anodes in sodium-ion batteries. The digitally designed ordered macropores enabled fast ion diffusion. The carbon framework electrode achieved an area capacity of 21.3 mAh cm^{-2} at a loading of 98 mg cm^{-2} (Figure 5a and b). Similarly, Sun et al.^[45] constructed a sulfur/carbon nanosphere cathode with a grid structure based on DIW. Uniformly distributed square pores worked as Li^+ transport channels and provided enough space for electrolyte accommodation. Consequently, the sulfur cathode with sulfur loading of 5.5 mg cm^{-2} delivered an initial discharge capacity of 1009 mAh g^{-1} and capacity retention of 87% after 200 cycles.

In these printed electrodes, the pore size will affect the mass transport and the active area in the electrode, further determining the performance. It can be precisely adjusted by

the printing periods.^[46] Zhang et al.^[47] prepared a porous Cu/C electrode with a series of customizable pore sizes (0.5–0.9 mm) by stereolithography. A decreased pore size in 3D-printed electrodes leaded to an increased active electrode surface area but an increased mass transfer resistance. When the electrode is used for thermally regenerated amino batteries, the power density of the battery has an initial increase and a subsequent decrease. The optimal pore size of electrode is 0.6 mm, and the corresponding maximum power density of the battery is up to 42.3 W m^{-2} .

It is important to emphasize here that these open periodic macropores are of great use in metal-air batteries, because they facilitate the fast flow and diffusion of the reactive gas. Additionally, the formed large three-phase reaction region facilitates the reaction of gas molecules and other active species and provides sufficient storage space for discharge products. The common surface passivation in conventional cathodes is also effectively avoided. For example, Sun et al.^[42] developed a graphene-based “ O_2 breathable” $\text{Na}-\text{O}_2$ cathode by a DIW process, which has continuous transport channels for O_2 , electrons, and sodium ions. In particular, the vertically open channels created by 3D printing promoted the diffusion and utilization of O_2 . The micrometer-sized pores between the graphene acted as electrolyte reservoirs and accommodated the discharge product (NaO_2). In addition, the interlinked graphene networks facilitated fast electron transport. Benefiting from these featured and advantages, the printed cathode showed satisfactory cycling stability over 120 cycles with a cutoff capacity of 500 mAh g^{-1} at 0.5 A g^{-1} .

However, it should be noted that electrochemical reactions usually occur at the nanoscale, which is far smaller than the resolution of 3D printing. Therefore, only relying on the 3D printing operation can not fully satisfy the customization requirements of electrode pore structure. Auxiliary pre-/post-processing is also an essential procedure for 3D printing

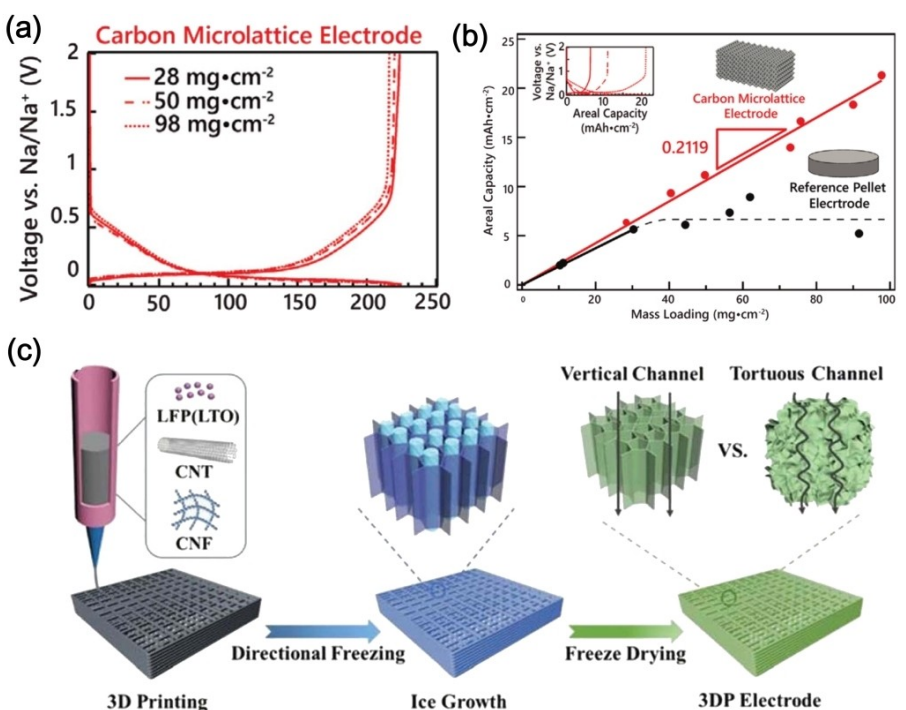


Figure 5. a) Battery performances of carbon micro-lattices at different mass loadings tested at 5 mA g^{-1} . b) Mass loading versus areal capacity plot of carbon micro-lattice electrodes and reference pellet electrodes. Reproduced with permission from Ref. [44]. Copyright (2022) Wiley-VCH. c) Schematic illustration of fabrication process of 3D printed electrodes with the directional freeze-drying treatment. Reproduced with permission from Ref. [50]. Copyright (2022) Wiley-VCH.

technology, which can make up for the shortcoming of low printing resolution. With the pre-/post-processing steps, the pore structure at a smaller scale can be created purposefully, including micropores, mesopores and macropores smaller than $1 \mu\text{m}$. Pre-processing refers to specifically creating pores in the raw materials prior to the printing operation. After printing, the existing pores are directly introduced into the electrode, helping to optimize the mass transport. Jin et al.^[48] pre-generated nanopores on the surface of reduced graphene oxide by oxidation etching method, and then developed an iron vanadate/reduced holey graphene oxide (FeVO/rHGO) cathode with a cellular structure by DIW for zinc-ion batteries. The generated hierarchical pore structures from periodic open macroporous channels to small nanopores enabled rapid electrolyte infiltration and large liquid-solid contact. One such a 3D-printed FeVO/rHGO cathode with mass loading of 24.4 mg cm^{-2} delivered a remarkable areal capacity of 7.04 mAh cm^{-2} at 6 mA cm^{-2} . After the printing process, a series of post-processing steps (heat treatment,^[19] template removal,^[49] freeze drying,^[50,51] etc.) are usually required to remove solvents and solidify structures. Reasonable selection and control of these post-processing methods can also accurately optimize the pore structure. Zhang et al.^[50] treated the printing electrode by directional freeze-drying, which created a large number of microscale vertical pores in the electrode. These pores had elongated morphology and penetrated the entire electrode from bottom to top (Figure 5c), largely shortening ion diffusion paths in the fiber radial direction. As expected, lithium ion battery composed of the

lithium iron phosphate cathode and the lithium titanate anode reached a high energy density (15.2 mWh cm^{-2}) and power density (75.9 mW cm^{-2}). Moreover, these directional pores helped to maintain favorable electrochemical stability even in the bending or compression states.

5. Customizable Architectures and Interfaces of Components

A full battery consists of several functional components, including anode, cathode, electrolyte, separator and current collector. The architectures of these functional components and their contact interfaces greatly influence the available reactive regions and the volumetric power/energy density. At the functional component level, 3D printing can realize customizable component architectures based on requirements and optimize their interface contact.

5.1. Electrode architectures

The architecture, size and configuration of the electrode on a spatial scale are strongly correlated with the performance.^[52] As mentioned above, 3D printing has a high design freedom and offers many opportunities to construct complex structures from microscopic to macroscopic levels. 3D printed batteries can break through the physical constraints and enable the custom-

izable electrode architectures and their configurations. More importantly, by advantage of the elaborate multi-scale structure and increased electrode active interface area, the battery can achieve both high power density and high areal energy density. In 3D printed electrode architectures, the most suitable choices include interdigititation, concentric micropillar arrays, 3D scaffolds and fibers, as shown in Figure 6(a-d).

5.1.1. Interdigititation

Interdigititation refers to electrodes with periodic finger-shaped or comb-shaped patterns on the same substrate. The cathode and the anode of the cell are paired together in interleaved mode. The narrow spaces between them are filled with electrolytes, which act as a medium for transporting ions. Two printed conductive wires are connected to an external circuit for the charging and discharging. In interdigitated structures, the critical factors affecting the electrochemical performance are the print spacing and the thickness and height of the electrodes. A smaller thickness of the electrodes and a shorter inter-separation distance means a larger active surface area and a shorter ion transport distance. In addition, the height of the

electrode increases linearly with the number of layers while the width remains almost constant in a layer-by-layer printing strategy. It contributes to a high areal capacity and a high-aspect ratio feature.^[53] In a representative work, lithium iron phosphate (LFP) and lithium titanate (LTO) inks (Figure 7a) with the desired rheological and printing behaviors are prepared.^[54] The high aspect ratio and multilayer LFP cathodes and LTO anodes were printed and assigned to the interdigitated architectures (Figure 7b). The resulting micro-battery, consisting of eight alternating layers of LTO and LFP, was shown to have a high areal capacity of $\sim 1.5 \text{ mAh cm}^{-2}$ with a cycle life of up to 30 cycles (Figure 7c).

The interdigitated structure has several advantages over the laminated structures. First, two opposing electrodes are inherently separated, eliminating the need for a separator,^[55] which simplifies manufacturing procedures, and avoids the risk of short circuits. Second, they offer a high degree of design freedom, and the size/shape of the cells and the areal capacity of the electrodes can be easily regulated. Third, the output current and voltage of planar interdigital batteries can be easily amplified due to their potential for miniaturization and integration, suggesting a wide range of potential applications in wearable electronics.^[56]

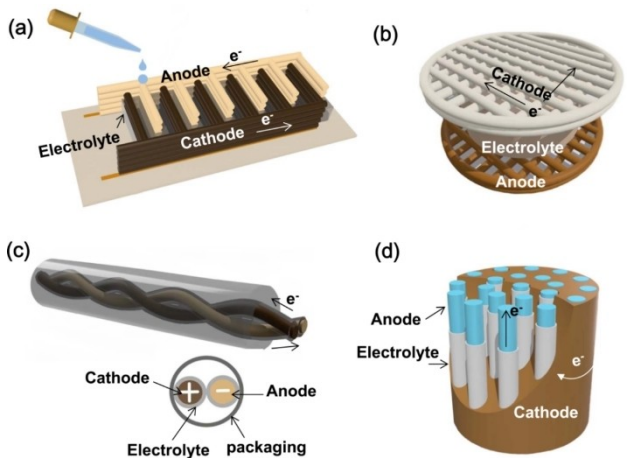


Figure 6. Schematic illustration of the common electrode architectures and their configurations: a) interdigititation, b) 3D scaffold, c) fibers and d) concentric micropillar array.

5.1.2. 3D scaffolds

3D-printed scaffold is a periodic micro-lattice composed of overlapping fine electrode filaments. The naturally interconnected pores between adjacent filaments form vertical open channels. Filament spacing can be easily adjusted by the printing periods.^[46] In the cell assembly, the cathode, electrolyte, separator and anode are stacked in sequence, and electrochemical measurements can be performed with coin cells. Due to their simple and efficient structure and good compatibility with test methods, 3D scaffolds are the most mentioned architectures for 3D printed electrode design.^[42,48]

Similar to the interdigitated structure, this 3D scaffold can also be applied to realize high mass loading electrodes. The difference is that the interdigitated structure increases the number of printing layers without changing the overall electrode thickness. In contrast, the 3D scaffold ensures the

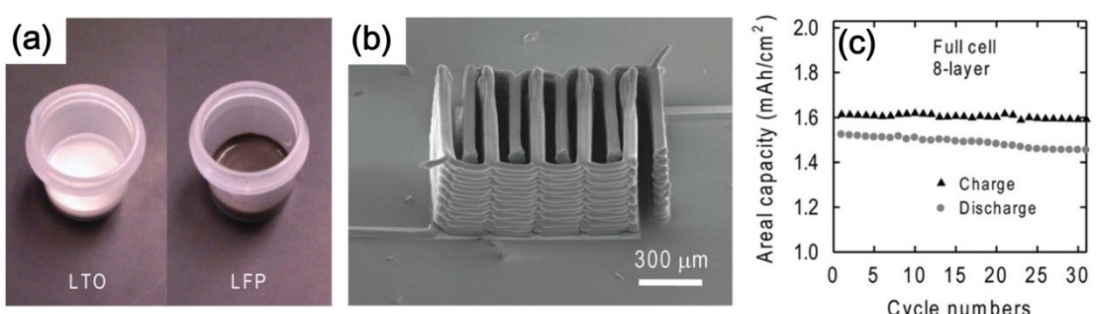


Figure 7. a) Digital images of LTO and LFP inks. b) Scanning electron microscopy (SEM) images of interdigititated LTO-LFP electrode architectures by DIW. c) Cycling performance and areal capacity of a full cell consisting of 8-layer interdigititated LTO-LFP electrodes. Reproduced with permission from Ref. [54]. Copyright (2013) Wiley-VCH.

bulk phase infiltration of the electrolyte in a thick electrode. For example, Chen et al.^[57] printed a 3D scaffold Li₄Ti₅O₁₂ electrode with a thickness of 1.09 mm and an areal mass loading of 39.44 mg cm⁻² by low temperature DIW. As shown in Figure 8(a–c), Li⁺ could transport through the vertically aligned pores instead of the tortuous paths inside the conventional electrodes, thereby decreasing the total transport distance of Li⁺. This electrode delivered an impressive areal capacity of 5.88 mAh cm⁻² at 0.1 C, corresponding an areal power density of 8.04 mW cm⁻². As a 3D conducting network, 3D scaffold has a larger active interface and a smaller local current density, which is very critical for the metal anode. Duan et al.^[58] combined stereolithography and electroless plating/electro-plating techniques to fabricate a multichannel Ni framework. When used as the 3D current collector, Ni frameworks achieved uniform electric field distribution and preferential homogeneous deposition of Zn (Figure 8d and e). Therefore, the full zinc-ion battery composed of polyaniline-intercalated vanadium oxide cathode and 3D Ni–Zn anode delivered an initial capacity of 314 mAh g⁻¹ even at the current density of 10 Ag⁻¹ and a high capacity retention of 80% after 1000 cycles.

5.1.3. Fiber

To meet the requirements of high flexibility and breathability for wearable electronics, the affiliated power sources need to be shrunk to a fiber form with small diameter (<10⁻³ m) and high aspect ratio (>10⁶).^[59] Fiber-shaped batteries could be

further twisted and woven into large-scale smart fabrics. Producing mechanically robust fiber-shaped electrodes is a prerequisite for the realization of fiber batteries, which is affected by the material composition and the fiber solidification method. The fibers are preferentially composed of materials with a high aspect ratio, such as carbon nanotubes and nanofibrillated cellulose, which are oriented in the axial direction with an interpenetrated structure.^[60] Besides, strong interaction (van der Waals forces^[61] and hydrogen bondings,^[62] etc.) between components can further improve the strength of the fiber electrodes. The extruded fibers can be solidified by direct drying^[63] or coagulation approach.^[64] From the perspective of the internal structure of the battery, the configurations of fiber batteries can be divided into parallel,^[63] twisted^[64] and coaxial.^[30,65] A parallel configuration means that the cathode and the anode are arranged in parallel on the same plane. In the twisted configuration, the cathode and the anode fibers covered with gel electrolyte are twisted into a bundle. The coaxial configuration, in which the cathode, electrolyte and anode are arranged in axial direction to form a core-shell architecture, is more complex. Using the DIW method, the researchers fabricated fiber-shaped LFP cathodes and LTO anodes, and twisted them together with a gel polymer electrolyte (Figure 9a).^[64] The as-printed fiber full battery showed a high initial discharge capacity of 110 mAh g⁻¹ (Figure 9b) and a good capacity retention of 81% over 30 cycles (Figure 9c). To improve the printing efficiency, Ji et al.^[63] developed a custom-built side-by-side nozzle, which can realize the one-step printing of electrodes and electrolytes with linear structures, as

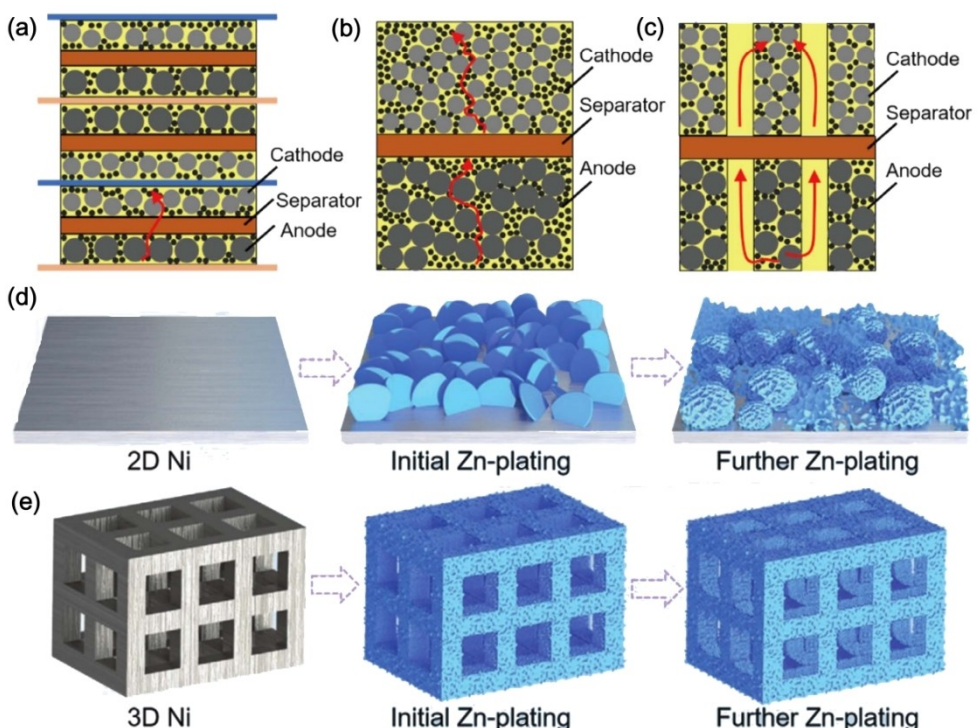


Figure 8. Charge delivery in a) thin conventional electrodes, b) thick conventional electrodes, and c) 3D grid porous electrodes. Reproduced with permission from Ref. [57]. Copyright (2022) Springer Nature. The corresponding schematic illustration of Zn deposition on the d) 2D Ni foil and e) 3D Ni scaffold. Reproduced with permission from Ref. [58]. Copyright (2021) Wiley.

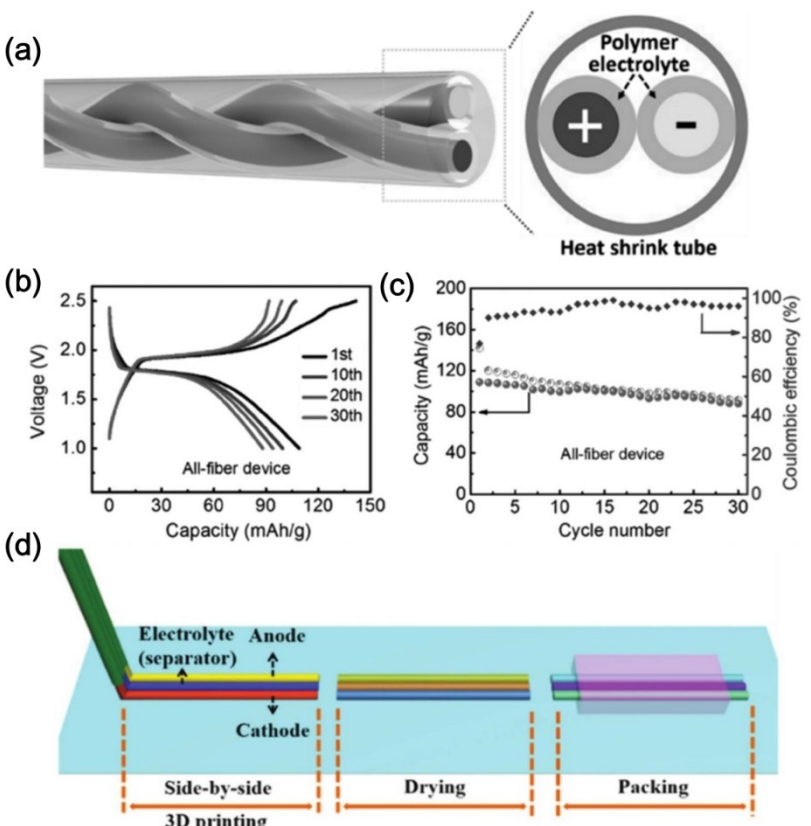


Figure 9. a) Schematic of an all-fiber LFP || LTO cell with a twisted configuration, and b) its corresponding charge/discharge curves and c) cycling performance. Reproduced with permission from Ref. [64]. Copyright (2017) Wiley. d) Schematic of the one-step side-by-side 3D printing process and the subsequent steps for fabricating a full battery. Reproduced with permission from Ref. [63]. Copyright (2022) Royal Society of Chemistry.

shown in Figure 9(d). The resulting electrode and electrolyte filaments had close contact interfaces. After subsequent drying, liquid electrolyte addition and encapsulation steps, a parallel linear battery was produced.

Fiber-shaped batteries have advantages in terms of miniaturization, adaptability, and weavability. The performance of fiber batteries depends on several parameters. For example, the fiber length can significantly affect the axial electron transport. The fiber diameter and the electrode/electrolyte interface contact are closely related to the transverse ionic transport.^[59] For future manufacturing and application of fiber batteries, several technical issues need to be solved, including large internal resistance, poor durability and difficult encapsulation and installation of separators.^[66]

5.1.4. Concentric micropillar array

In the microelectronics industry, the size of devices is constantly decreasing, and thus the required size of the battery is on the order of 1–10 mm³, and the footprint on the substrate is only a few tens of square millimeters. Concentric micropillar arrays are a novel class of 3D micro-battery configurations with uniformly distributed and vertically aligned electrode posts. A uniform electrolyte film covers the electrode surface, and the remaining space is filled with the active material of the counter

electrode. Each post coupled with the surrounding electrolyte and counter electrode forms an entire cell unit, and all units are connected in parallel.^[67] Evenly spaced electrode posts are usually produced by etching and electro-deposition, such as silicon anodes.^[13] D. Golodnitsky et al.^[68] developed a prototype concentric micro-battery by FDM. A perforated polymer substrate was first printed, and then a three-layered structure of LiFeO₄ cathode, electrolyte and LiTi₅O₁₂ anode was fabricated by the electrophoretic deposition (Figure 10a). The obtained areal energy density of the 3D concentric micro-battery on the printed polymer substrate is three times higher than that of the commercial planar thin-film battery, with the same power capacity per battery footprint (Figure 10b).

With such a concentric micropillar array, it is possible to simultaneously achieve high energy and power density due to the large mass loading and small ion diffusion distances. It covers a small footprint area, which is also well suited for device miniaturization. Despite these advantageous features, the development of concentric micropillar arrays still faces some serious fabrication challenges. One challenge is the implementation of a conformal electrolyte coating on the surface of the electrode posts. The coated electrolyte layer not only needs to insulate the cathode and the anode to avoid short circuits, but also should have thin and homogeneous properties to achieve efficient ion transport. The fabrication of concentric micropillar arrays is a complex and costly process.

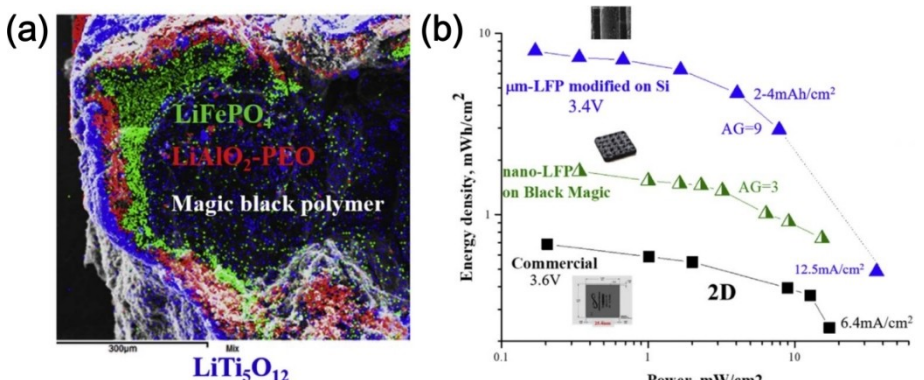


Figure 10. a) Cross-sectional elemental mapping of tri-layer structures ($\text{LiFePO}_4\text{-LiAlO}_2\text{-PEO-LiTi}_5\text{O}_{12}$) deposited on 3D printed conducting polymer substrate (Magic black polymer in the picture); b) Ragone plot comparing electrochemical performance of 3D micro-batteries on 3D-printed-polymer substrates with commercial thin-film planar battery and 3D $\text{LiFePO}_4\text{/Li}$ batteries on perforated-silicon. Reproduced with permission from Ref. [68]. Copyright (2018) Elsevier.

5.2. Electrolyte architecture and interface

As an essential component in a battery, the electrolyte plays a role in transporting ions between the cathode and the anode. Generally, electrolytes can be divided into three categories: liquid, gel-polymer and ceramics electrolytes.^[69] Liquid electrolytes could be injected directly into the devices, but their low-flash-point property compromises the safety of the batteries.^[70] Applications of gel-polymer and ceramics electrolytes would effectively address this issue. However, gel-polymer and ceramics electrolytes are deficient in electrical conductivity and mechanical properties, which are closely related to their bulk phase architecture and composition. 3D printing enables the purposeful design of a variety of structures and components. For example, hybrid electrolytes offer the possibility of integrating the properties of ceramics and gel-polymer electrolytes. However, ion transport across the electrolyte is largely hindered by the formation of multiple interfaces. Bruce et al.^[71] created a 3D bi-continuous structured hybrid electrolyte by stereolithography, consisting of bi-continuous conducting ceramic $\text{Li}_{1.4}\text{Al}_{0.4}\text{Ge}_{1.6}(\text{PO}_4)_3$ and insulating epoxy polymer. The ceramic provided high ionic conductivity, while the polymer provided suitable mechanical properties. The results showed that the printed micro-architectures (cube, gyroid, diamond, and bijel-derived) had obvious effects on the electrical and mechanical properties of the electrolytes. The gyroid structures filled with epoxy give excellent ionic conductivity of $1.6 \times 10^{-4} \text{ S cm}^{-1}$ at room temperature and superior mechanical properties.

The nature of solid-solid contact between the electrolyte and the electrode increases resistance at the interface. 3D printing can reduce impedance by enhancing interface contact, as well as increasing interface contact area.^[72] Deiner et al.^[73] realized a smooth, conformal, and nonporous polymer electrolyte composed of polyethylene oxide (PEO), lithium difluoro(oxalato)borate (LiDFOB), and alumina nanoparticles by AJP. The printing process is performed directly on LiFePO_4 cathode and enable the polymer electrolyte to penetrate fully into the electrode bulk. The resulting electrode/electrolyte interface had a low resistance. At a C/15 rate, batteries with this

AJP printed electrolyte had a specific capacity of 85 mAh g^{-1} at 45°C and 162 mAh g^{-1} at 75°C . In the most cases, additional processing steps are required to remove the solvent and template, which easily causes deformation and instability in the printed electrolyte and deteriorates interfacial contact. To overcome this issue, Shahbazian-Yassar et al.^[72] used an elevated-temperature DIW method to fabricate hybrid solid-state electrolytes consisting of a polymer matrix and a ceramics-liquid electrolyte. Strikingly, a thin and dense interlayer was formed between the electrolyte and the electrode, resulting in a significantly reduced interfacial resistance of the solid-state batteries.

Conventionally, solid-state electrolytes are used in the form of planar geometries and random porosities, resulting in a high cell area specific resistance.^[74] Wachsman et al.^[75] developed two kinds of $\text{Li}_x\text{La}_3\text{Zr}_2\text{O}_{12}$ (LLZO) solid electrolyte ink, including "conformal" and "self-supporting" inks. Based on these two inks, a series of thin, non-planar, and intricate electrolyte architectures were developed, and the influence of structural properties of the electrolyte-electrode interface on the performance was investigated (Figure 11a and b). Using a printed LLZO stacked array as the electrolyte, a symmetrical Li metal battery was fabricated and tested. Galvanostatic cycling (Figure 11c) showed that low interfacial impedance is exhibited due to the close interface contact and increased contact area.

5.3. Current collectors and separators

In addition to the electrodes and electrolytes, other components include the current collector and separator. These inactive parts are also critical to ensure stability and performance. The current collector is used to collect and transfer electrons between the active material layer and the external circuit. In 3D printed batteries, highly conductive metal inks (Au ,^[54] Ag ,^[76] Cu ,^[77] and Ni ,^[78]) have often been printed to create usable current collectors. For example, Wang et al.^[78] developed a transform-printing strategy to produce an interdigitated Au/Ni current collector by combining stereolithography with electroless deposition (Figure 12a). This novel fabrication meth-

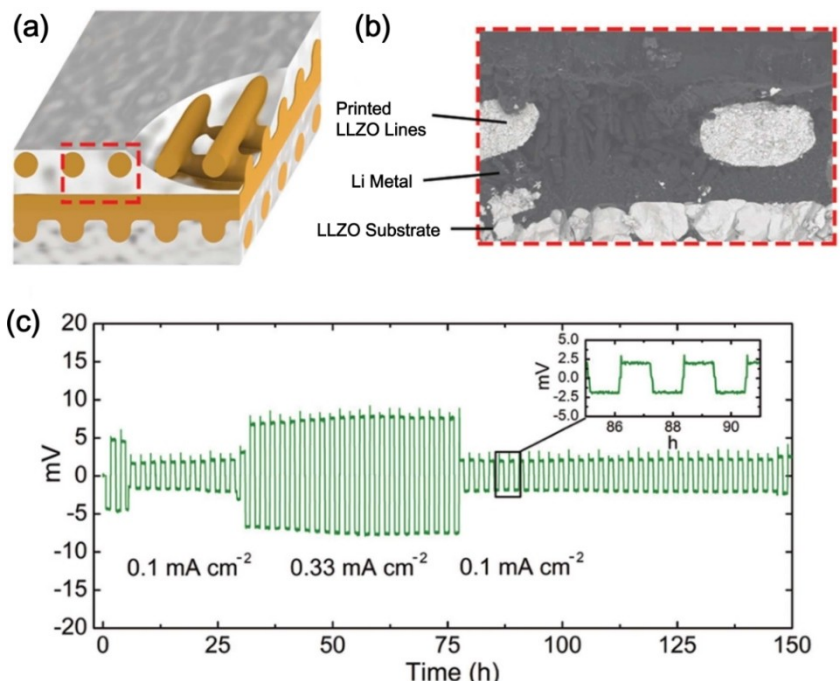


Figure 11. a) Schematic of a symmetric Li metal battery, in which Li was filled in pores between 3D-printed LZZO grids with a stacked-array pattern on a LZZO substrate. b) Cross-sectional SEM of the 3D-printed LZZO|Li metal interface (red line). c) Galvanostatic cycling of the Li|3D-printed LZZO|Li metal battery at different current densities. Each plating/stripping cycle was 1 h long. Reproduced with permission from Ref. [75]. Copyright (2018) Wiley-VCH.

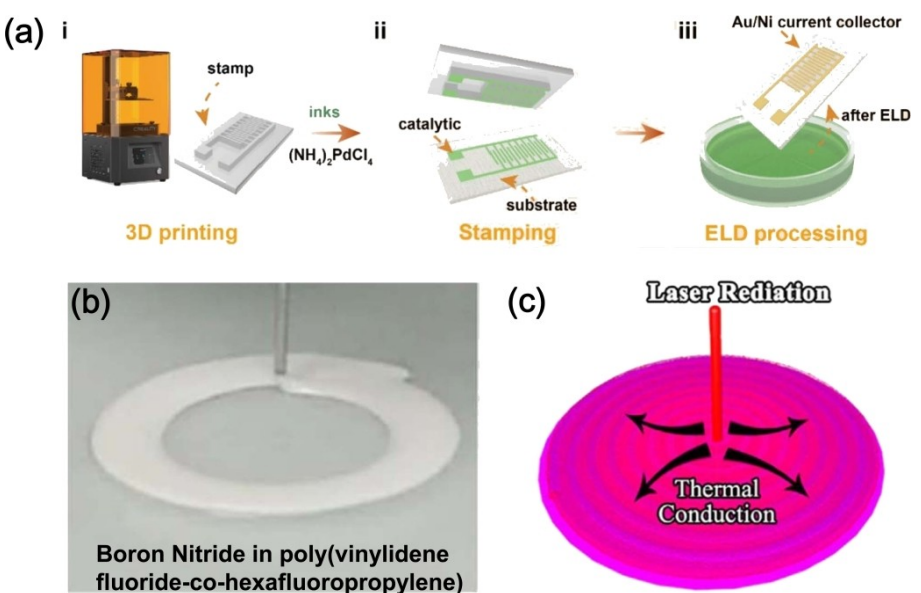


Figure 12. a) Schematic illustration of the fabrication process of metal current collector: i) 3D printing resin stamps; ii) stamping catalysts for electroless deposition; iii) depositing metals. b) Digital image of the printing process of a thermal management separator. Reproduced with permission from Ref. [78]. Copyright (2022) Elsevier. c) Schematic of heat dissipation from the center of the boron nitride-separator when exposed to local heat source. Reproduced with permission from Ref. [81]. Copyright (2018) Elsevier.

od was compatible with both paper and plastic substrates, and the resulting Au/Ni pattern had good mechanical flexibility. Based on this metal current collector, an aqueous Zn-MnO₂ micro-battery exhibited an energy density of 168 $\mu\text{Wh cm}^{-2}$ at a power density of 0.18 mW cm^{-2} . In these printed current collectors, Au and Ag metals are commonly used in order to improve electronic conductivity. However, the high cost limits

their large-scale applications,^[79] so the development of low-cost non-noble metal current collectors, such as highly conductive graphene, carbon nanotubes, MXenes and non-noble metals, by 3D printing methods is needed.

The common raw materials of 3D printed separators are ceramic-filled polymer composites, such as Al₂O₃/nanofibrillated cellulose,^[62] Al₂O₃/ethoxylated trimethylolpropane

triacylate,^[80] SiO₂/poly(methyl methacrylate),^[63] etc. Furthermore, the functional role of the prepared separator can be extended by specific functional materials into printable inks. For example, Hu et al.^[81] integrated boron nitride nanosheets into poly(vinylidene fluoride-co-hexafluoropropylene) and prepared printable inks. DIW technique was used to fabricate a thermal management separator consisting of a spiral pattern (Figure 12b). Due to the excellent thermal properties of BN, the resulting separator was able to realize rapid heat dissipation and uniform heat distribution (Figure 12c). When it was used in Li metal batteries, this separator facilitated homogeneous Li nucleation and suppressed dendrite growth. The Li||Li symmetric cells using this thermal management separator showed extremely stable cycling with a lower overpotential over 500 h.

6. Customizable Mechanical Deformability and Appearance

Different application scenarios have specific requirements for the shape and mechanical deformation ability of battery. Therefore, customization is also required at the cell level. For example, batteries in e-skins and electronic fabrics are expected to be resistant to bending and stretching. This presents demands on the printed structures that can buffer or counteract the effects of these external operations. For example, Lee et al.^[82] mixed natural graphite and LiNi_{0.6}Co_{0.2}Mn_{0.2}O₂ with carbon fiber and binder to prepare printable inks, respectively. The DIW method was proposed to produce fibrous electrodes. A twisted yarn-type LIB was then fabricated by twisting the separator-coated anode and cathode fibers together in a heat-shrinkable tube. The device exhibited a specific capacity of 166 mAh g⁻¹ at 0.1 C and could withstand a great deal of bending. These yarn-type LIBs have been incorporated into commercial fabrics and show promise for wearable devices. Li et al.^[62] developed a stretchable LIB by DIW. The good stretchability of the batteries was attributed to the strong bonding between the nanofibrillated cellulose and carbon nanotubes used, and the elaborate customizable serpentine structure. The printed cell showed a reversible stretchability of 50%.

The appearance of battery is a more intuitive part of customization. Many object surfaces are not flat but curved or even irregularly undulating, such as organs, skin, or arms. When the battery can be embedded and fit into these non-flat surfaces, which is known as conformal printing, there is no need for a dedicated battery storage location and the space utilization is greatly increased. Conformal printing imposes higher requirements on the printing technology, including printing precision, control flexibility, and packaging difficulty. Pan et al.^[26] realized the non-flat printing of electrodes (LFP cathode and LTO anode) with arbitrary shape and adjustable thickness by means of AJP. The printed electrodes were packaged in the PVDF-based package and a customizable non-planar LIB was obtained (Figure 13a). Compared to the planar full battery, this non-planar battery showed a favorable specific

capacity of 135 mAh g⁻¹ with very little capacity loss (Figure 13b and c).

For a qualified external package, it is necessary to focus on its electrochemical stability, compatibility and air/moisture hermeticity.^[26] To reflect the mechanical deformation capability of the electrode, plastic and elastomeric tube or film is often used as the external packaging.^[64,83] However, these packaging components are poorly fitted to the electrodes and have a fixed shape. For this reason, 3D printing takes advantage of its ability of customizable manufacturing, creating external packages on demand. Lewis et al.^[37] used stereolithography to print polymer packages in arbitrary geometries for zinc-ion batteries, such as rectangular, cylindrical, H- and ring-shapes. Combined with electrospinning and laser micro-machining techniques, the required shaped cathode, anode, and separator are fabricated and filled into customizable packages. The integrated zinc-ion batteries demonstrated high power performance and have been used in wearable photosensors.

7. Conclusion and Perspective

As an advanced manufacturing technology, 3D printing is driving the further development of customizable batteries. In terms of the manufacturing process, 3D printing significantly simplifies the production process and reduces costs. From an application of view, 3D printing is advantageous for realizing miniaturized and customizable target devices. Future batteries could be manufactured and tailored according to common usage scenarios and desired features. However, the large-scale production and commercial application of customizable batteries through 3D printing is still immature, and the main challenges cover four aspects, including inks and materials, printing techniques, architectural design and fully printed devices (Figure 14).

7.1. Exploring printable inks and materials.

The preparation of printable inks or materials is an essential prerequisite for 3D printing. Compatible inks or materials have completely different properties for different printing methods. For DIW, the high viscosity inks need to have good shear-thinning properties to ensure their smooth flow through the nozzle. The properties of the prepared inks are very sensitive to the concentration, particle size, composition, and their percentages. For the IJP and AJP, the ideal inks should have a lower viscosity and consist of free-agglomerating nanometer particles to avoid nozzle clogging. For the VPP and FDM, their printing materials do not need to be prepared into viscoelastic inks, but there are specific requirements for the material properties. FDM requires thermoplastic materials, while VPP requires materials that can be polymerized under ultraviolet light. However, these materials are generally electrochemically inert.

Although much research has been done on 3D printed batteries, especially for the electrode components, the active materials currently available are limited. Most of the studies still

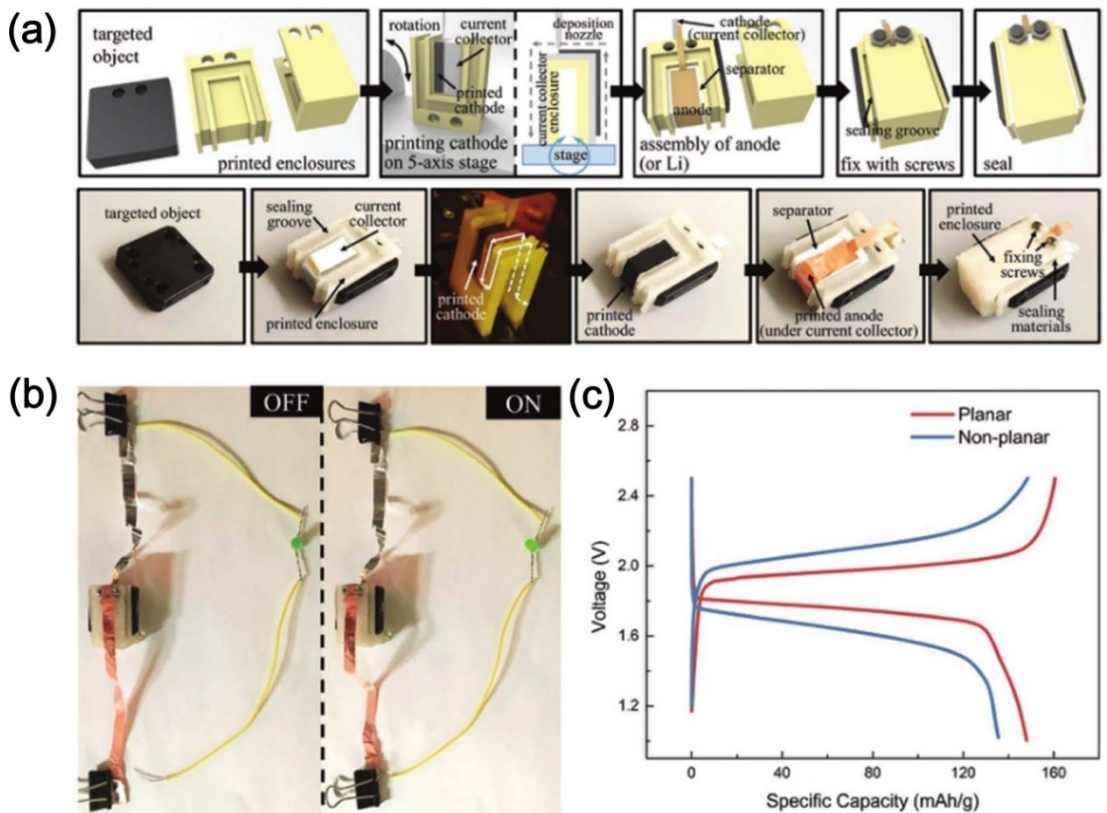


Figure 13. a) Schematics and photographs of the design and assembly process of a customizable non-planar LIB. b) Photographs of the non-planar packaged half-cell illuminating a green LED. c) Charge/discharge curves of the planar and non-planar packaged full cells. Reproduced with permission from Ref. [26]. Copyright (2019) Wiley-VCH.

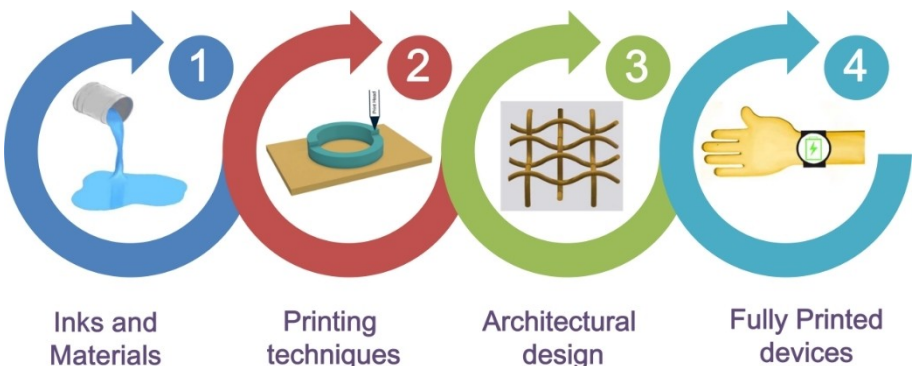


Figure 14. Key challenges in the printing of customizable batteries.

choose LTO and LFP as electrode materials due to their minimal volumetric expansion^[84] and remarkable thermal stability,^[85] and the practical energy density of the fabricated device is limited. Therefore, it is necessary to exploit superior inks containing active materials with higher capacitance. In addition, for the manufacturing of separators, electrolytes, current collectors and packaging, there are few compatible printable materials and inks. Therefore, new printable materials and inks still need to be developed for components other than electrodes.

7.2. Optimizing 3D printing techniques.

Higher resolution 3D printing technologies provide greater accuracy and more precise structural control, which is conducive to the production of miniaturized batteries. Unfortunately, the maximum technical resolution of current 3D printing technology is limited to the micron scale.^[13] Low printing resolution severely limits the use of 3D printing in complex battery microstructures. To solve this problem, multidisciplinary collaboration is required, including mechanical design, automation control, chemistry, and materials. 4D printing is an

extended technique of 3D printing, which has one more "Dimension" (time) than 3D printing. The 4D printed structure can change its shape, property or functionality with time under the external stimuli, such as temperature, pressure, light, etc.^[86,87] Although 4D printing has not yet been applied to battery manufacturing, it is expected to realize more smart battery devices in the future, in line with the rapid development of wearable electronics.

7.3. Demand-driven architectural design of customizable batteries

The outstanding advantage of 3D printing is that it can achieve a variety of battery component architecture, and also transform the laminated configuration into 3D configuration. The produced large active interface and large ion transport channel greatly boost cell performance. For the future architectural design, three points need to be paid special attention to. According to the requirements on the device shapes and mechanical properties in specific application scenarios, future research needs to further expand the architecture types, such as stretchable spring structure, fractal motif and origami structure. Most of the current literature reports are limited to the performance tests of the single sample and structure. The relationship between electrode/electrolyte architecture parameters and mechanical/electrochemical performance lacks systematically investigated. For this purpose, advanced finite element simulation or other numerical simulation methods could be employed to simulate and screen the optimized architecture design. The auxiliary pre-/post-processing can make up for the low resolution of 3D printing, and create the meso and nanopores, but their ability to customize the pore size, shape and distribution is limited. Future research is needed to refine these pre-/post-processing techniques and improve their customization capabilities.

7.4. Implementing fully 3D printed and packaged batteries.

Currently, most studies focus on a single part of the battery, but their integration into sophisticated 3D architectures and final fabrication into full 3D batteries has been neglected. There are two main reasons for this difficulty. First, a fully packaged battery consists mainly of cathode, anode, electrolyte, current collector, separator, and packaging. The material composition and properties of these components are completely different, and include inorganic nanoparticles, polymers, and metals. The applicable printing techniques for each component are completely different. Second, good interfacial contacts between battery functional components are essential for low interfacial resistance but are difficult to achieve under practical operating conditions. In view of these problems, the integration of different printing technologies into one system will be necessary in the future. The system can enable one-step or step-by-step customizable manufacturing of batteries. Meanwhile, printing inks for different battery components require in-

depth research and systematic control to ensure the interface consistencies during the solidification or curing process.

Despite the above challenges, 3D printing is still considered to be one of the revolutionary and imaginative technologies for customizable batteries. It offers much greater design freedom and has almost eliminated all the conventional slurry-coating manufacturing steps. In the future, the production of customizable batteries will be more intelligent and more customer-oriented.

Acknowledgements

The work was supported by the Natural Science Foundation of Shandong Province, China (No. ZR2021QE098), and Postdoctoral Science Foundation of China (No. 2022M712329).

Conflict of Interests

The authors declare no conflict of interest.

Keywords: 3D printing • battery appearance • component architecture • customizable batteries • flexible batteries,

- [1] S. Zeadally, F. K. Shaikh, A. Talpur, Q. Z. Sheng, *Renewable Sustainable Energy Rev.* **2020**, *128*, 109901.
- [2] R. Kumar, J. Shin, L. Yin, J. M. You, Y. S. Meng, J. Wang, *Adv. Energy Mater.* **2016**, *7*, 1602096.
- [3] D. Son, J. Kang, O. Vardoulis, Y. Kim, N. Matsuhisa, J. Y. Oh, J. W. To, J. Mun, T. Katsumata, Y. Liu, A. F. McGuire, M. Krason, F. Molina-Lopez, J. Ham, U. Kraft, Y. Lee, Y. Yun, J. B. Tok, Z. Bao, *Nat. Nanotechnol.* **2018**, *13*, 1057–1065.
- [4] M. Walter, M. V. Kovalenko, K. V. Kravchyk, *New J. Chem.* **2020**, *44*, 1677–1683.
- [5] J. Piątek, S. Afyon, T. M. Budnyak, S. Budnyk, M. H. Sipponen, A. Slabon, *Adv. Energy Mater.* **2020**, *11*, 2003456.
- [6] Y. Liu, R. Zhang, J. Wang, Y. Wang, *iScience* **2021**, *24*, 102332.
- [7] T. Chu, S. Park, K. Fu, *Carbon Energy* **2021**, *3*, 424–439.
- [8] Y. Pang, Y. Cao, Y. Chu, M. Liu, K. Snyder, D. MacKenzie, C. Cao, *Adv. Funct. Mater.* **2019**, *30*, 1906244.
- [9] M. R. Nichols, *Met. Powder Rep.* **2019**, *74*, 257–258.
- [10] S. C. Joshi, A. A. Sheikh, *Virtual Phys. Prototyp.* **2015**, *10*, 175–185.
- [11] W. D. Zhou, J. S. Chen, *Mater. Sci. Forum* **2018**, *913*, 558–563.
- [12] H. Dodziuk, *Kardiachir Torakochirurgia Pol.* **2016**, *13*, 283–293.
- [13] Z. Lyu, G. J. H. Lim, J. J. Koh, Y. Li, Y. Ma, J. Ding, J. Wang, Z. Hu, J. Wang, W. Chen, Y. Chen, *Joule* **2021**, *5*, 89–114.
- [14] T. D. Ngo, A. Kashani, G. Imbalzano, K. T. Q. Nguyen, D. Hui, *Composites Part B* **2018**, *143*, 172–196.
- [15] J. A. Lewis, *Adv. Funct. Mater.* **2006**, *16*, 2193–2204.
- [16] A. Shahzad, I. Lazoglu, *Composites Part B* **2021**, *225*, 109249.
- [17] S. Tagliaferri, A. Panagiotopoulos, C. Mattevi, *Mater Adv* **2021**, *2*, 540–563.
- [18] K. Fu, Y. Wang, C. Yan, Y. Yao, Y. Chen, J. Dai, S. Lacey, Y. Wang, J. Wan, T. Li, Z. Wang, Y. Xu, L. Hu, *Adv. Mater.* **2016**, *28*, 2587–2594.
- [19] L. Zeng, H. N. He, H. Y. Chen, D. Luo, J. He, C. H. Zhang, *Adv. Energy Mater.* **2022**, *12*, 2103708.
- [20] M. Saadi, A. Maguire, N. T. Pottackal, M. S. H. Thakur, M. M. Ikram, A. J. Hart, P. M. Ajayan, M. M. Rahman, *Adv. Mater.* **2022**, *34*, 2108855.
- [21] Y. Yang, W. Yuan, X. Q. Zhang, Y. H. Yuan, C. Wang, Y. T. Ye, Y. Huang, Z. Q. Qiu, Y. Tang, *Appl. Energy* **2020**, *257*, 114002.
- [22] J. P. Mensing, T. Lomas, A. Tuantranont, *Sustain. Energy Fuels* **2020**, *25*, 00190.
- [23] M. Singh, H. M. Haverinen, P. Dhagat, G. E. Jabbour, *Adv. Mater.* **2010**, *22*, 673–85.

- [24] A. Mahajan, C. D. Frisbie, L. F. Francis, *ACS Appl. Mater. Interfaces* **2013**, *5*, 4856–64.
- [25] R. Rodriguez, L. J. Deiner, B. H. Tsao, J. P. Fellner, *ACS Appl. Energ. Mater.* **2021**, *4*, 9507–9512.
- [26] X. Yu, Y. Liu, H. Pham, S. Sarkar, B. Ludwig, I. M. Chen, W. Everhart, J. Park, Y. Wang, H. Pan, *Adv. Mater. Technol.* **2019**, *4*, 1900645.
- [27] O. A. Mohamed, S. H. Masood, J. L. Bhowmik, *Adv. Manuf.* **2015**, *3*, 42–53.
- [28] P. Wang, B. Zou, *Coating* **2022**, *12*, 827.
- [29] K. Rajan, M. Samyako, K. Kadirkama, W. S. W. Harun, M. M. Rahman, *Int. J. Adv. Manuf. Tech.* **2022**, *120*, 1531–1570.
- [30] H. Ragones, A. Vinegrad, G. Ardel, M. Goor, Y. Kamir, M. M. Dorfman, A. Gladikh, D. Golodnitsky, *J. Electrochem. Soc.* **2019**, *167*, 070503.
- [31] C. Reyes, R. Somogyi, S. Niu, M. A. Cruz, F. Yang, M. J. Catenacci, C. P. Rhodes, B. J. Wiley, *ACS Appl. Energ. Mater.* **2018**, *1*, 5268–5279.
- [32] A. Maurel, M. Courty, B. Fleutot, H. Tortajada, K. Prashantha, M. Armand, S. Gruegeon, S. Panier, L. Dupont, *Chem. Mater.* **2018**, *30*, 7484–7493.
- [33] X. Zhang, K. Zhang, L. Zhang, W. Wang, Y. Li, R. He, *Mater. Des.* **2022**, *215*, 110470.
- [34] A. Maurel, A. C. Martinez, S. Gruegeon, S. Panier, L. Dupont, P. Cortes, C. G. Sherrard, I. Small, S. T. Sreenivasan, E. Macdonald, *IEEE Access* **2021**, *9*, 140654–140666.
- [35] Y. He, S. Chen, L. Nie, Z. Sun, X. Wu, W. Liu, *Nano Lett.* **2020**, *20*, 7136–7143.
- [36] C. Li, J. J. Du, Y. Gao, F. Bu, Y. H. Tan, Y. X. Wang, G. W. Fu, C. Guan, X. Xu, W. Huang, *Adv. Funct. Mater.* **2022**, *32*, 2205317.
- [37] C. Kim, B. Y. Ahn, T. S. Wei, Y. Jo, S. Jeong, Y. Choi, I. D. Kim, J. A. Lewis, *ACS Nano* **2018**, *12*, 11838–11846.
- [38] A. A. Gupta, M. C. M. Soer, M. Taherzadeh-Sani, S. G. Cloutier, R. Izquierdo, *IEEE T. Comp. Pack. Man.* **2019**, *9*, 2482–2489.
- [39] A. Maurel, S. Gruegeon, B. Fleutot, M. Courty, K. Prashantha, H. Tortajada, M. Armand, S. Panier, L. Dupont, *Sci. Rep.* **2019**, *9*, 18031.
- [40] X. Wu, S. Xia, Y. Huang, X. Hu, B. Yuan, S. Chen, Y. Yu, W. Liu, *Adv. Funct. Mater.* **2019**, *29*, 1903961.
- [41] Z. Wang, Z. Huang, H. Wang, W. Li, B. Wang, J. Xu, T. Xu, J. Zang, D. Kong, X. Li, H. Y. Yang, Y. Wang, *ACS Nano* **2022**, *16*, 9105.
- [42] X. Lin, J. Wang, X. Gao, S. Wang, Q. Sun, J. Luo, C. Zhao, Y. Zhao, X. Yang, C. Wang, R. Li, X. Sun, *Chem. Mater.* **2020**, *32*, 3018–3027.
- [43] J. Cai, J. Jin, Z. Fan, C. Li, Z. Shi, J. Sun, Z. Liu, *Adv. Mater.* **2020**, *32*, 2005967.
- [44] Y. Katsuyama, A. Kudo, H. Kobayashi, J. Han, M. Chen, I. Honma, R. B. Kaner, *Small* **2022**, *18*, 2202277.
- [45] X. Gao, Q. Sun, X. Yang, J. Liang, A. Koo, W. Li, J. Liang, J. Wang, R. Li, F. B. Holness, A. D. Price, S. Yang, T.-K. Sham, X. Sun, *Nano Energy* **2019**, *56*, 595–603.
- [46] F. Zhang, K. Wu, X. Xu, W. Wu, X. Hu, K. Yu, C. Liang, *Energy Technol.* **2021**, *9*, 2100628.
- [47] P. Chen, Y. Shi, L. Zhang, J. Li, X. Zhu, Q. Fu, Q. Liao, *Ind. Eng. Chem. Res.* **2020**, *59*, 21286–21293.
- [48] H. Ma, X. Tian, T. Wang, K. Tang, Z. Liu, S. Hou, H. Jin, G. Cao, *Small* **2021**, *17*, 2100746.
- [49] X. Mu, T. Bertron, C. Dunn, H. Qiao, J. Wu, Z. Zhao, C. Saldana, H. J. Qi, *Mater. Horiz.* **2017**, *4*, 442–449.
- [50] X. Li, S. Ling, L. Zeng, H. He, X. Liu, C. Zhang, *Adv. Energy Mater.* **2022**, *12*, 2200233.
- [51] L. Qian, H. F. Zhang, *J. Chem. Technol. Biotechnol.* **2011**, *86*, 172–184.
- [52] J. Wang, Q. Sun, X. Gao, C. Wang, W. Li, F. B. Holness, M. Zheng, R. Li, A. D. Price, X. Sun, T. K. Sham, X. Sun, *ACS Appl. Mater. Interfaces* **2018**, *10*, 39794–39801.
- [53] J. Li, M. C. Leu, R. Panat, J. Park, *Mater. Des.* **2017**, *119*, 417–424.
- [54] K. Sun, T. S. Wei, B. Y. Ahn, J. Y. Seo, S. J. Dillon, J. A. Lewis, *Adv. Mater.* **2013**, *25*, 4539–43.
- [55] M. Cheng, R. Deivanayagam, R. Shahbazian-Yassar, *Batteries & Supercaps* **2020**, *3*, 130–146.
- [56] K. Brousse, P. L. Taberna, P. Simon, *J. Electrochem. Soc.* **2022**, *169*, 070534.
- [57] C. Y. Liu, Y. Qiu, Y. L. Liu, K. Xu, N. Zhao, C. S. Lao, J. Shen, Z. W. Chen, *J. Adv. Ceram.* **2022**, *11*, 295–307.
- [58] G. Zhang, X. Zhang, H. Liu, J. Li, Y. Chen, H. Duan, *Adv. Energy Mater.* **2021**, *11*, 2003927.
- [59] T. Khudiyev, B. Grena, G. Loke, C. Hou, H. Jang, J. Lee, G. H. Noel, J. Alain, J. Joannopoulos, K. Xu, J. Li, Y. Fink, J. T. Lee, *Mater. Today* **2022**, *52*, 80–89.
- [60] Y. Li, H. Zhu, Y. Wang, U. Ray, S. Zhu, J. Dai, C. Chen, K. Fu, S. H. Jang, D. Henderson, T. Li, L. Hu, *Small Methods* **2017**, *1*, 1700222.
- [61] Z. Xu, C. Gao, *Nat. Commun.* **2011**, *2*, 571.
- [62] J. Qian, Q. Chen, M. Hong, W. Xie, S. Jing, Y. Bao, G. Chen, Z. Pang, L. Hu, T. Li, *Mater. Today* **2022**, *54*, 18–26.
- [63] J. Ding, H. Zheng, X. Ji, *Chem. Commun.* **2022**, *58*, 5241–5244.
- [64] Y. Wang, C. Chen, H. Xie, T. Gao, Y. Yao, G. Pastel, X. Han, Y. Li, J. Zhao, K. K. Fu, L. Hu, *Adv. Funct. Mater.* **2017**, *27*, 1703140.
- [65] D. Ji, H. Zheng, H. Zhang, W. Liu, J. Ding, *Chem. Eng. J.* **2022**, 433.
- [66] F. Mo, G. Liang, Z. Huang, H. Li, D. Wang, C. Zhi, *Adv. Mater.* **2020**, *32*, 1902151.
- [67] Y. Horowitz, E. Strauss, E. Peled, D. Golodnitsky, *Isr. J. Chem.* **2021**, *61*, 38–50.
- [68] E. Cohen, S. Menkin, M. Lifshits, Y. Kamir, A. Gladikh, G. Kosa, D. Golodnitsky, *Electrochim. Acta* **2018**, *265*, 690–701.
- [69] F. Zheng, M. Kotobuki, S. Song, M. O. Lai, L. Lu, *J. Power Sources* **2018**, *389*, 198–213.
- [70] P. Isken, C. Dippel, R. Schmitz, R. W. Schmitz, M. Kunze, S. Passerini, M. Winter, A. Lex-Balducci, *Electrochim. Acta* **2011**, *56*, 7530–7535.
- [71] S. Zekoll, C. Marriner-Edwards, A. K. O. Hekselman, J. Kasemchainan, C. Kuss, D. E. J. Armstrong, D. Cai, R. J. Wallace, F. H. Richter, J. H. J. Thijssen, P. G. Bruce, *Energy Environ. Sci.* **2018**, *11*, 185–201.
- [72] M. Cheng, Y. Jiang, W. Yao, Y. Yuan, R. Deivanayagam, T. Foroozan, Z. Huang, B. Song, R. Rojaee, T. Shokuhfar, Y. Pan, J. Lu, R. Shahbazian-Yassar, *Adv. Mater.* **2018**, *30*, 1800615.
- [73] L. J. Deiner, T. Jenkins, T. Howell, M. Rottmayer, *Adv. Eng. Mater.* **2019**, 21.
- [74] D. Zhang, X. Xu, Y. Qin, S. Ji, Y. Huo, Z. Wang, Z. Liu, J. Shen, J. Liu, *Chemistry* **2020**, *26*, 1720–1736.
- [75] D. W. McOwen, S. Xu, Y. Gong, Y. Wen, G. L. Godbey, J. E. Gritton, T. R. Hamann, J. Dai, G. T. Hitz, L. Hu, E. D. Wachsman, *Adv. Mater.* **2018**, *30*, 1707132.
- [76] K. Tang, H. Ma, Y. Tian, Z. Liu, H. Jin, S. Hou, K. Zhou, X. Tian, *Virtual Phys. Prototyp.* **2020**, *15*, 511–519.
- [77] A. Maurel, H. Kim, R. Russo, S. Gruegeon, M. Armand, S. Panier, L. Dupont, *Front. Energy Res.* **2021**, *9*, 651041.
- [78] R. G. Haoran Wang, H. Li, J. Wang, C. Du, X. Wang, Z. Zheng, *Chem. Eng. J.* **2022**, *429*, 132196.
- [79] Y. Gu, J. Federici, *Batteries* **2018**, *4*, 42.
- [80] T. S. Wei, B. Y. Ahn, J. Grotto, J. A. Lewis, *Adv. Mater.* **2018**, *30*, 1703027.
- [81] Y. Liu, Y. Qiao, Y. Zhang, Z. Yang, T. Gao, D. Kirsch, B. Liu, J. Song, B. Yang, L. Hu, *Energy Storage Mater.* **2018**, *12*, 197–203.
- [82] S. Praveen, G. S. Sim, C. W. Ho, C. W. Lee, *Energy Storage Mater.* **2021**, *41*, 748–757.
- [83] X. Fang, W. Weng, J. Ren, H. Peng, *Adv. Mater.* **2016**, *28*, 491–6.
- [84] X. Zhang, W. Shyy, A. M. Sastry, *J. Electrochem. Soc.* **2007**, *154*, A910–A916.
- [85] S. Y. Chung, J. T. Bloking, Y. M. Chiang, *Nat. Mater.* **2002**, *1*, 123–8.
- [86] F. Momeni, S. M. Hassani, N. X. Liu, J. Ni, *Mater. Des.* **2017**, *122*, 42–79.
- [87] J. Lee, H.-C. Kim, J.-W. Choi, I. H. Lee, *Int. J. Precis. Eng. Manuf.-Green Technol.* **2017**, *4*, 373–383.

Manuscript received: April 17, 2023

Revised manuscript received: May 3, 2023

Accepted manuscript online: May 4, 2023

Version of record online: May 16, 2023